

## Surfactant-like Behavior of Short-Chain Alcohols in Porphyrin Aggregation

Maria Angela Castriciano,<sup>†</sup> Maria Grazia Donato,<sup>‡</sup> Valentina Villari,<sup>‡</sup> Norberto Micali,<sup>\*,‡</sup> Andrea Romeo,<sup>§</sup> and Luigi Monsù Scolaro<sup>\*,§,||</sup>

CNR-Istituto per lo Studio dei Materiali Nanostrutturati, Salita Sperone 31, I-98166 Vill. S. Agata, Messina, Italy, CNR-Istituto per i Processi Chimico-Fisici, Salita Sperone, Contrada Papardo, Faro Superiore, 98158 Messina, Italy, and Dipartimento di Chimica Inorganica, Chimica Analitica e Chimica Fisica and C.I.R.C.M.S.B., Università di Messina, Salita Sperone 31, 98166 Vill. S. Agata, Messina, Italy

Received: April 14, 2009; Revised Manuscript Received: June 29, 2009

UV/vis absorption and time-resolved fluorescence measurements on alcoholic solutions of meso-tetrakis(4-sulfonatophenyl)porphyrin (TPPS<sub>4</sub>) in neutral and acid form have been performed as a function of the alcohol polarity. These solutions show a peculiar behavior that mimics porphyrin in confined water solutions. In alcohols, TPPS<sub>4</sub> exhibits a metastable phase showing the formation of new species in analogy with the confined water environment of AOT microemulsions. Various species have been detected at different pH values and on aging the solutions. Under neutral pH conditions, the porphyrin is present as free base monomer (S415) with a small amount of H-dimeric species (S400). On aging, the S415 leads to the formation of a new species (S423), which has been assigned as a J-type dimer of the neutral porphyrin. The species S400 and S423 are not present in bulk water solution but are typical of TPPS<sub>4</sub> in confined water. On decreasing pH, the S415 almost immediately converts into the diacid form (S438), which evolves toward red-shifted J-aggregates (S490) and blue-shifted H-aggregates (S420). On decreasing alcohol polarity, the kinetic evolution from fresh to aged solution and from the monomeric diacid species to H- and J-aggregates speeds up. Exploiting the amphiphilic character of short chain alcohols and widely varying their polarity, we were able to enhance in bulk conditions the peculiar behavior observed in close proximity to the microemulsion wall.

## Introduction

Water-soluble meso-tetrakis(4-sulfonatophenyl)porphyrin (TPPS<sub>4</sub>) at neutral pH values is present in solution as a monomeric free base. In acidic solution ( $pK_a = 4.9$ ),<sup>1,2</sup> its zwitterionic diacid form is present with a Soret band bathochromically shifted ( $\Delta\lambda = +16$  nm) with respect to the neutral form. Under strongly acidic conditions,<sup>1–9</sup> this diacid species leads to J-aggregates, characterized by peculiar structural and photophysical properties. Such aggregates exhibit a lateral arrangement of porphyrins, which form a linear array stabilized by strong electrostatic interactions between the peripheral negatively charged sulfonate groups and the protonated core of the macrocycle, as well as by hydrogen bonding and van der Waals forces. The strong electronic coupling between porphyrins determines relevant effects both on absorption bands (bathochromic shift  $\Delta\lambda \approx +50$  nm) and in the electromagnetic scattering.<sup>10–14</sup> The mesoscopic structure obtained by fostering aggregation with acids can be tuned from fractal to nanorods by acting on the intermolecular interaction potential. A fine control of the rod length as function of porphyrin concentration has been obtained.<sup>15</sup>

Porphyrin aggregates have been also obtained in micellar phase with different kind of surfactants.<sup>16–18</sup> In microemulsion confined aqueous solution, TPPS<sub>4</sub> porphyrin shows a completely different behavior with respect to the bulk solution. Various species have been detected as a function of the size of the

microemulsions, concentration of the porphyrin, pH, and aging of the samples.<sup>19</sup> In this confined water pool (nanoreactor), the size of the aggregate can be controlled; however, the removal of the continuous phase (oil) causes the macroscopic aggregation of TPPS<sub>4</sub>.<sup>19,20</sup>

Despite many reports on aggregation phenomena in aqueous or mixed aqueous–organic phase, very few investigations have been devoted to study both neutral and acidic alcoholic environments.<sup>21,22</sup> An amphiphilic cosurfactant behavior is typical for long chain alcohols, while some properties of short chain alcohols could be discussed in term of amphiphilic model system. In particular, methanol–water mixtures exhibit the same thermodynamic nonideality of surfactant solutions, showing a tendency to self-organize<sup>23–28</sup> with hydrophobic-like structures supported by the nonpolar group interactions. Thus, methanol has been used as a prototypical amphiphilic system. In this framework, the use of alcohol as solvent for porphyrin can provide an environment able to mimic in bulk the microemulsion experimental conditions. Furthermore, the employment of solvents less polar than water can affect the size and the structure of TPPS<sub>4</sub> aggregates that are mainly stabilized by the occurrence of strong electrostatic interactions and hydrogen bonds. As already reported for apolar solvents,<sup>29</sup> a decrease of the medium polarity largely enhances the involved interactions strength, affecting the structural arrangement of the chromophores in the supramolecular assemblies. Here, we report a spectroscopic and photophysical characterization of TPPS<sub>4</sub> in alcohols with decreasing polarity from methanol ( $\epsilon_r = 33$ ) to 2-propanol ( $\epsilon_r = 18$ ). The systems have been investigated under different experimental conditions (neutral/acidic and aging of the samples). By exploiting the amphiphilic character of short chain alcohols, we succeeded in obtaining, in bulk conditions, new TPPS<sub>4</sub>

\* To whom correspondence should be addressed. E-mail: (N.M.) micali@me.cnr.it; (L.M.S.) lmonsu@unime.it.

<sup>†</sup> CNR-Istituto per lo Studio dei Materiali Nanostrutturati.

<sup>‡</sup> CNR-Istituto per i Processi Chimico-Fisici.

<sup>§</sup> Università di Messina.

<sup>||</sup> Also CNR-Istituto per lo Studio dei Materiali Nanostrutturati.

species similar to those already observed in confined micro-emulsion water pools. Furthermore, unlike TPPS<sub>4</sub> J-aggregates in aqueous solution for which fluorescence emission is strongly quenched, the aggregation process in methanol leads to the formation of nanosized J-aggregates still retaining fluorescence emission.

## Experimental Section

**Materials.** The meso-tetrakis(4-sulfonatophenyl)porphyrin sodium salt TPPS<sub>4</sub> was purchased from Aldrich Co. The stock solutions, obtained by dissolving the solid porphyrin in alcohols (methanol, ethanol, 1-propanol, and 2-propanol from Lab-Scan Ltd., spectrophotometric grade), were stored in the dark and used within a week from preparation. The nominal concentration ( $3 \times 10^{-6}$  M) used in our experiments was determined spectrophotometrically by using the molar extinction coefficient at the Soret band maximum in water ( $\varepsilon_{414\text{nm}} = 5.33 \times 10^5 \text{ M}^{-1} \text{ cm}^{-1}$ ).<sup>1</sup> Because of the low solubility of TPPS<sub>4</sub> in 1- and 2-propanol, micromolar solutions in these solvents have been obtained after at least 24 h of magnetic stirring at room temperature. In order to exclude the influence of small amounts of adventitious water inevitably present (specially in methanol), intentional doping by water has been performed; no effect has been detected in the final system.

**Experimental Setup.** UV/vis spectra were carried out on a Hewlett-Packard model 8453 diode array spectrophotometer using 1 cm path length quartz cells. Fluorescence emission and light scattering (LS) experiments (as a function of wavelength) were performed on a Jasco model FP-750 spectrofluorimeter. For LS measurements, a synchronous scan protocol with a right angle geometry has been adopted.<sup>30</sup> LS spectra were not corrected for the absorption of the samples. Static (SLS) and quasi-elastic light scattering (QELS) measurements were performed by using an experimental setup based on a Malvern 4700 submicrometer particle analyzer system.<sup>31</sup> Time resolved fluorescence measurements have been carried out by a time-correlated-single-photon-counting (TCSPC)<sup>32</sup> homemade apparatus. An Ar<sup>+</sup> laser, operating in the mode-locked regime at a repetition rate of 82 MHz, synchronously pumps a Rhodamine 6G dye laser, providing  $\sim 580$  nm polarized excitation pulses with a pulse duration of  $\sim 2$  ps fwhm. Fluorescence photons have been detected (at 90°) through a rotating analyzer, a monochromator, a long pass filter, and microchannel plate photomultiplier. A nonlinear least-squares iterative deconvolution procedure based on the Marquardt algorithm has been used to analyze the collected data. In this way, a resolution better than 50 ps is obtained. Time-resolved fluorescence, UV-vis, and light scattering measurements have been carried out at temperature of 300 K.

**Methods.** In general, the time dependence of the total fluorescence intensity can be described by a multiexponential decay; fluorescence lifetimes  $\tau_i$  and their relative amplitudes  $\alpha_i$  (with  $\sum_i \alpha_i = 1$ ) can be obtained by fitting data according to the following multiexponential decay law<sup>33,34</sup>

$$I(t) = I_0 \sum_i \alpha_i \exp(-t/\tau_i) \quad (1)$$

By using the analyzer it is possible to measure the anisotropy of fluorescence emission defined as

$$r(t) = \frac{I_{\text{VV}}(t) - I_{\text{VH}}(t)}{I_{\text{VV}}(t) + 2I_{\text{VH}}(t)} = \frac{D(t)}{S(t)} \quad (2)$$

The parameters describing the fluorescence anisotropy decay have been obtained through a two-step procedure.<sup>33,34</sup> At first time  $S(t)$  was analyzed, using a reconvolution procedure based on the multiexponential model, to obtain the parameter  $\alpha_i \tau_i$  and,  $I_0$  of total fluorescence decay

$$S(t) = I(t) = I_0 \sum_i \alpha_i \exp(-t/\tau_i) \quad (3)$$

Afterward, the difference  $D(t)$  was fitted considering a simple-exponential decay of the fluorescence anisotropy:

$$D(t) = S(t)r(t) = S(t)r_0 \exp(-t/\theta_R) = I_0 r_0 \exp(-t/\theta_R) \times \sum_i \alpha_i \exp(-t/\tau_i) \quad (4)$$

where  $r_0$  is the anisotropy in absence of rotational diffusion and  $\theta_R$  is the rotational correlation time. In some cases, an additive constant  $r_\infty$  to  $r(t)$  was introduced to take into account a long decay contribution due to static interaction with large clusters. The goodness of the fit has been evaluated on the basis of the reduced chi-square values (typically close to unity for all the decay curves) and of the residual plots, ensuring that the latter are randomly distributed. In the case of a mixture of different fluorophores, or for a single fluorophore in different environments, each fluorophore population displays its own intensity and anisotropy decay. For this associated system the overall anisotropy decay is an intensity-weighted linear function of the anisotropy of each component (or in each environment).<sup>33</sup> By assuming that each species  $m$  displays a single lifetime  $\tau_m$  and rotational correlation time  $\theta_m$ , the anisotropy decay is

$$r(t) = \frac{\sum_m f_m(t) r_m(t)}{\sum_m \alpha_m \exp(-t/\tau_m)} = \frac{\sum_m \alpha_m \exp(-t/\tau_m) r_{0m} \exp(-t/\theta_{Rm})}{\sum_m \alpha_m \exp(-t/\tau_m)} \quad (5)$$

where  $r_m(t)$  is the anisotropy decay in each environment (or of each component) and  $f_m(t)$  is the fractional intensity of the  $m$ -th component at any time  $t$ .

In the case of resonance scattering, to avoid the effect of the scattered light on the position and broadening of the absorption J-band, a dissection of scattering and absorption contributes has been done by a simple method that is based on two independent measurements of extinction and RLS on the same sample and a linear regression analysis of the data in the region close to the resonance.<sup>35</sup>

## Results and Discussion

**Neutral Fresh Solutions.** TPPS<sub>4</sub> is readily soluble in methanol and ethanol, displaying (Figure 1) a very sharp and intense B band centered at 415 nm (S415), accompanied by four weaker Q bands (512, 548, 590, and 645 nm) and a shoulder at 400 nm in the absorption spectra. The light scattered by the samples is comparable to that of the net solvents and decreases in correspondence with the absorption bands of the samples

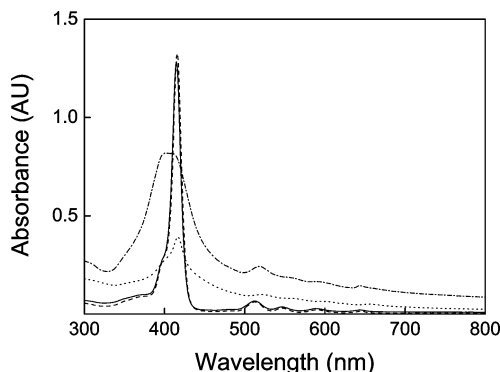


**Figure 1.** UV/vis spectra of TPPS<sub>4</sub> in the following various alcohol solutions: methanol (solid line), ethanol (dashed line), 1-propanol, (dotted line), and 2-propanol (dashed-dotted line).

**TABLE 1: Summary of the Time-Resolved Fluorescence Measurements<sup>a</sup>**

sample	$\tau_1$	$\tau_2$	$\tau_3$	$\alpha_1$	$\alpha_2$	$\alpha_3$	$\theta_R$	$r_0$	$r_\infty$	$\lambda_{em}$
methanol		1.7	9.9		32	68	0.3	0.06	0	650
ethanol		0.9	11		39	61	0.5	0.04	0	650
1-propanol	0.08	1.6	3.8	99.6	0.3	0.1	0.86	0.2	0.03	620
	0.21	1.5	6	64	30	6	1.1	0.12	0.02	655
2-propanol	0.29	1	5.4	60	39	1	6	0.1	0	655

<sup>a</sup> Lifetimes are expressed in nanoseconds, wavelength in nanometers, and the relative amplitude  $\alpha$  in percent. The experimental error on  $\tau_1$  is 0.05 ns, on  $\tau_2$  is 0.1 ns, on  $\tau_3$  is 0.5 ns, on  $\theta_R$  is 0.1 ns, on  $r_0$  is 0.02, and on  $r_\infty$  is 0.01.

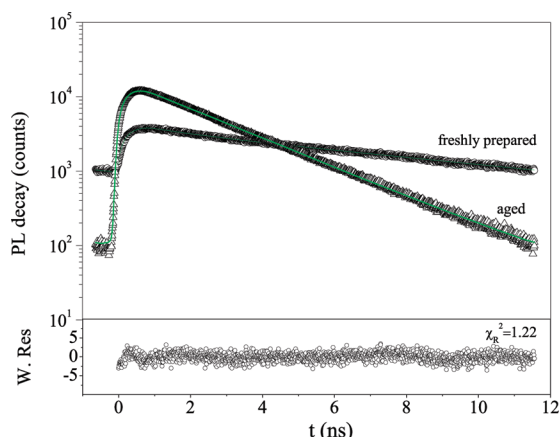


**Figure 2.** Time-resolved fluorescence decay of TPPS<sub>4</sub> in methanol solution. Fresh solution,  $\lambda_{em} = 640$  nm; aged solution,  $\lambda_{em} = 660$  nm. The lowest part of the plot shows typical weighted residuals of the fit.

(namely, no resonance effects are observed). Solutions are strongly fluorescent, showing the two emission bands typical of this porphyrin (650 and 716 nm). Time-resolved fluorescence results are reported in Table 1. The fluorescence decays show a biexponential behavior with a main component exhibiting a long lifetime close to 10 ns (Figure 2), ascribable to the presence in solution of TPPS<sub>4</sub> free base S415. The second component with a short lifetime close to 1 ns can be associated to the presence of a small amount of dimers or oligomers.

The fluorescence anisotropy decays ( $r(t)$ ) are reported in Table 1 and in Figure 3 (top) and Figure 4 (top). The rotational correlation times measured in ethanol (0.5 ns) and methanol (0.3 ns) properly scale with the viscosity of the solvents, suggesting their attribution to the same species in solution. In this regard, since in our experimental conditions a zero initial anisotropy value ( $r_0$ ) for the monomer in aqueous solution has

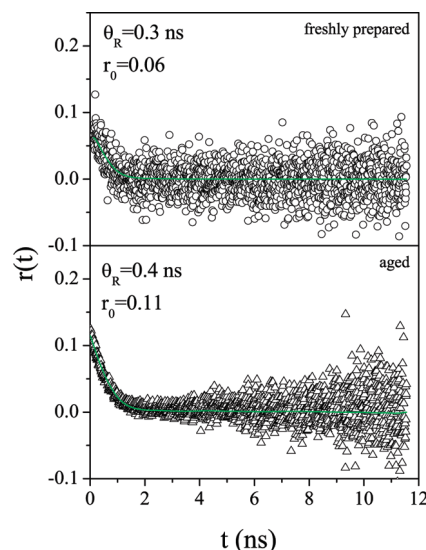


**Figure 3.** Time resolved anisotropy decays of TPPS<sub>4</sub> in methanol solution. Fresh solution,  $\lambda_{em} = 640$  nm; aged solution,  $\lambda_{em} = 660$  nm. The values of the rotational correlation times  $\theta_R$  and of the initial anisotropy  $r_0$  are also indicated.

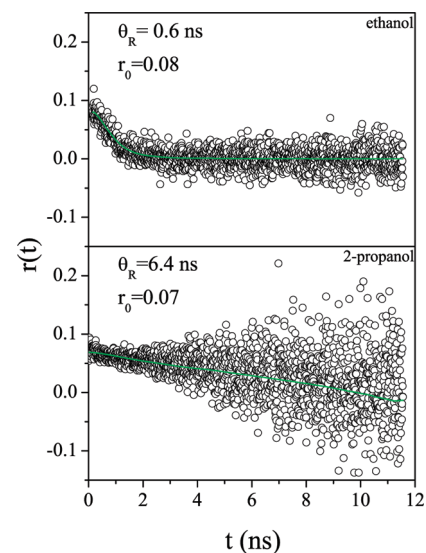


**Figure 4.** Time resolved anisotropy decay of TPPS<sub>4</sub> in ethanol ( $\lambda_{em} = 650$  nm) and 2-propanol ( $\lambda_{em} = 655$  nm) solutions. The values of the rotational correlation times  $\theta_R$  and of the initial anisotropy  $r_0$  are also indicated.

been already reported,<sup>19,34,36</sup> we associate the observed correlation times to a small amount of dimeric species,<sup>21</sup> which contributes to the quenched component of the fluorescence intensity decay. However, in other literature reports<sup>6</sup> for a different excitation wavelength an initial anisotropy  $r_0 \neq 0$  for the monomer in aqueous solutions has been observed.

In 1-propanol and 2-propanol, which are less polar than methanol and ethanol, the solubility of the porphyrin is reduced. The UV/vis spectra of the solutions (Figure 1) exhibit very broad absorption bands. Moreover, a large light scattering background due to the presence of non-dissolved porphyrin has been detected in both cases as confirmed by the increase of the elastically scattered light in the LS spectra. The absence of a resonance light scattering (RLS) peak in the absorption region leads us to exclude the presence in solution of well organized chromophore aggregates.<sup>37</sup> The absorption spectra of TPPS<sub>4</sub> in both 1- and 2-propanol solutions display a Soret band at 416 nm (S415) and four Q-bands at 520, 560, 602, and 656 nm, together with



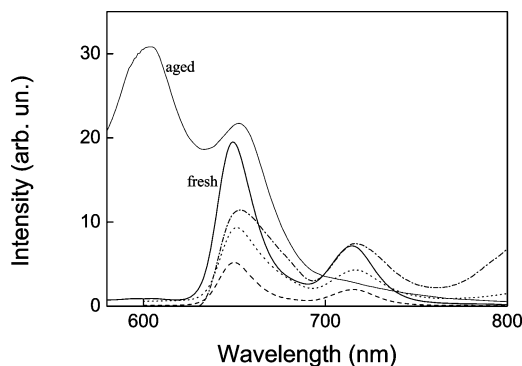


**Figure 5.** Fluorescence emission spectra of TPPS<sub>4</sub> in the following various alcoholic solutions: methanol (solid line, fresh and aged solution), ethanol (dashed line), 1-propanol, (dotted line), and 2-propanol (dashed-dotted line);  $\lambda_{\text{ex}} = 424$  nm. (The increasing signal around 800 nm is due to the second order diffraction of the monochromator grating.)

a contribution centered at 400 nm (S400). In 2-propanol solution, this latter band exhibits an absorbance value comparable to that of the Soret band. The emission spectra (Figure 5) show the usual two-banded profile centered at 651 and 716 nm in 1-propanol and bathochromically shifted ( $\Delta\lambda = +2$  nm) in 2-propanol solution. Moreover, in the latter case, broader bands with respect to the other solvents have been detected. The time-resolved fluorescence emission shows a quite different scenario with respect to the methanol and ethanol solutions. The fluorescence decays ( $\lambda_{\text{em}} = 655$  nm) have been fitted according to a three-exponential profile and the results have been collected in Table 1. The two principal emitting components have lifetime values of some hundreds of picoseconds and close to 1 ns, whereas low relative amplitude of few percent exhibits a longer lifetime of about 6 ns. The clear identification of the different species in solution through the steady-state fluorescence spectra is prevented by the strong scattered light, which does not allow for the estimation of the absorption contribution in the excitation spectra. Anyway, the high amplitude of subnanosecond lifetime component and the strong background in the extinction spectra suggest the existence of some porphyrin clusters in solution, probably due to the low solubility in these solvents. The nanosecond lifetime components are related to the presence of dimeric or oligomeric species (S400), also confirmed by the long rotational correlation times (1.1 and 6 ns for 1- and 2-propanol, respectively) as obtained by the fluorescence anisotropy decays measurements.

The species S400 observed in all these alcoholic solutions has been already reported for this porphyrin in a confined environment close to the wall of a microemulsion<sup>19</sup> and it has been associated to a H-dimer of TPPS<sub>4</sub>.<sup>16</sup>

**Neutral Aged Solutions.** The alcoholic solutions of TPPS<sub>4</sub> show a metastable phase and evolve in time toward the final species S423 faster as the polarity of the solvent is lowered. As widely reported,<sup>2,6,15,19</sup> TPPS<sub>4</sub> micromolar solutions show a spectroscopic behavior that is not affected by aging both in neutral aqueous solutions and apolar solvents.<sup>29</sup> On the contrary, in the confined environment of microemulsion water pools, the system shows some typical spectral changes upon aging, identified with the formation of a H-dimeric species of the diacid porphyrin.<sup>19</sup> We report results on the system with the slowest kinetics (namely, methanol solution); in any case, a similar behavior is observed also in ethanol, 1- and 2-propanol solutions. The huge amount of the S400 species (not evolving toward the S423 species) in these two latter alcohols, together with

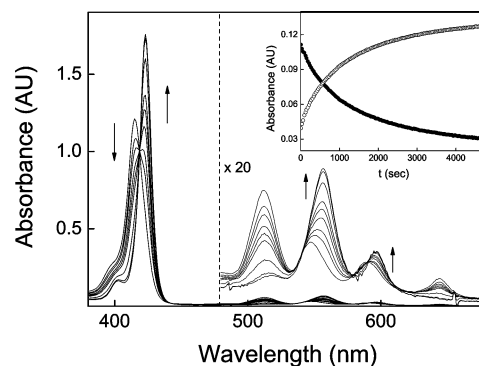


**Figure 6.** UV-vis spectral changes on aging TPPS<sub>4</sub> methanol solution (scanning time 600 s). In the inset, the corresponding UV-vis kinetic profile is reported (decreasing profile,  $\lambda_{\text{ex}} = 414$  nm; increasing profile,  $\lambda_{\text{ex}} = 423$  nm).

the lower yield of conversion (due to the decreased polarity of the solvents), leads us to choose the methanol solution as the best system to follow the aging effect.

On standing the TPPS<sub>4</sub> in methanol solution, the UV-vis spectra display the gradual disappearance of the B-band at 415 nm (S415) with the formation of a new band at 423 nm (S423), together with two Q-bands at 557 and 598 nm (Figure 6). The time dependence of the absorbance of this new band, bathochromically shifted with respect to the Soret band of the free base S415, displays an exponential profile, as reported in the inset of Figure 6, although the kinetic rate of formation of S423 is largely variable from a couple of hours to one month, depending on the aging of the stock solution. In any case, the observed final component is the S423 species that does not further evolve with time. This pattern of behavior is very similar to what already was observed on aging the same porphyrin into microemulsion water pools.<sup>19</sup> The presence of two Q-bands is an indicator of the increased symmetry of the porphyrin core, going from  $D_{2h}$  to  $D_{4h}$ .

In microemulsion water pool, the increased symmetry suggested the protonation of the porphyrin core, which was further supported by the experimental conditions imposed by the confinement (i.e., local pH and ionic strength). Thus, the observed hypsochromic shift with respect to the diacid Soret band (434 nm) was attributed to the formation of the H-type dimer of the diacid porphyrin.

In methanol solution, we can rule out the protonation of the porphyrin core and the influence of the ionic strength on the arrangement of the TPPS<sub>4</sub> monomers. Thus, the formation of a diacid species can be excluded and the observed bathochromic shift with respect to the monomer species S415 can be safely associated to the formation of a J-type dimer of the porphyrin free base. The increased symmetry could be justified by the formation of hydrogen bonds involving the nitrogen cores and the negatively charged sulfonate groups present in the periphery of the ring. This process is expected to be largely enhanced in low-polarity solvents with respect to water, as already reported for apolar solvents.<sup>29</sup>

The emission spectrum of the final S423 species (Figure 5) shows two blue-shifted bands (605 and 653 nm) with respect to the fresh porphyrin-methanol solution. The fluorescence emission decay correspondent to the two emission bands have been well fitted with a triexponential curve (see Table 2). In these aged samples, the almost totality of the relative amplitude (>99%) is due to a very short-living component with a lifetime value close to the experimental resolution. The interconversion kinetic between the different species, observed in UV/vis spectra,

**TABLE 2: Summary of the Time-Resolved Fluorescence Measurements of Aged Porphyrin Methanol Solution<sup>a</sup>**

aging	$\tau_1$	$\tau_2$	$\tau_3$	$\alpha_1$	$\alpha_2$	$\alpha_3$	$\theta_R$	$r_0$	$r_\infty$	$\lambda_{em}$
2 day		1.5	9.9		45	55	0.39	0.05	0	650
10 days		1.4	9		63	37	0.27	0.07	0.01	650
2 months	0.075	1.3	4.6	99.4	0.5	0.1	0.35	0.14	0	625
		1.4	8.5		66	34	0.25	0.08	0	650
5 months	0.04	2	>11	>99	<1	<1	0.32	0.11	0	610
	0.07	2	10	>99	<1	<1	0.31	0.12	0	655

<sup>a</sup> Time units and experimental errors are the same as in Table 1.

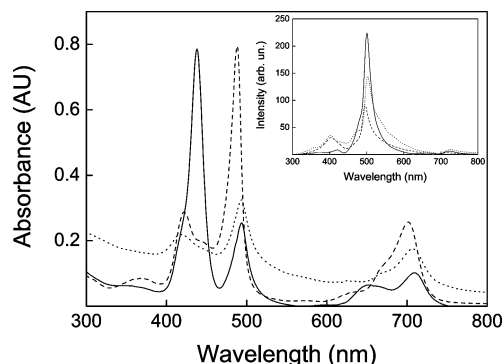


**Figure 7.** UV/vis spectra of the TPPS<sub>4</sub> J-aggregates in the following various acidic alcoholic solutions: methanol (solid line), ethanol (dashed line), and 1-propanol (dotted line). In the inset, the corresponding RLS spectra are shown.

is also evident from a gradual increase of the apparent initial fluorescence anisotropy from approximately  $r_0 = 0.06$  in the freshly made to  $r_0 = 0.12$  in the aged solutions. In fact, if a mixture of monomeric species (a) and aggregated form (b) is taken into account, the associated anisotropy decay is  $r(t) = r_a(t)f_a(t) + r_b(t)f_b(t)$ . As the anisotropy decay of the single porphyrin molecule never has been observed with our experimental setup, only the aggregated form contributes to the initial associated anisotropy. Thus, from the ratio between the observed anisotropy and the fractional intensity of the aggregated form, approximately the same anisotropy value  $r_{0b} = 0.12 \pm 0.02$  is calculated for aggregated species in methanol at all aging. Such value is in fair agreement with the value reported by Maiti et al.<sup>6</sup> ( $r_0 = 0.15$ ) for the initial anisotropy of the dimeric TPPS<sub>4</sub> in aqueous solutions.

**Acidic Species.** UV/vis absorption spectroscopy and time-resolved fluorescence emission point out that, as mentioned above, in neutral alcoholic solutions various species are present depending on the polarity of the solvents and the aging of the samples. On adding HCl vapors to the TPPS<sub>4</sub> neutral alcohol solutions, the UV/vis spectra (Figure 7) show the instantaneous formation of a Soret band at approximately 438 nm (S438) slightly bathochromically shifted with respect to the more polar aqueous solutions. In addition, the presence of only two Q-bands points to the formation of the diacid porphyrin. S438 eventually interconverts to a final species with a narrow peak bathochromically shifted to 490 nm (S490), accompanied by a broader one hypsochromically shifted (S420) with respect to the Soret band of the diacid porphyrin and by a series of three Q-bands. The RLS spectra (inset of Figure 7) show an intense and sharp peak in close proximity of the absorption band (490 nm), indicating the presence of porphyrin J-aggregates in solution.

Whereas in aqueous solution we were not able to collect the fluorescence signal of J-aggregate<sup>38</sup> with our experimental apparatus, in alcoholic solutions it is clearly observable, due to

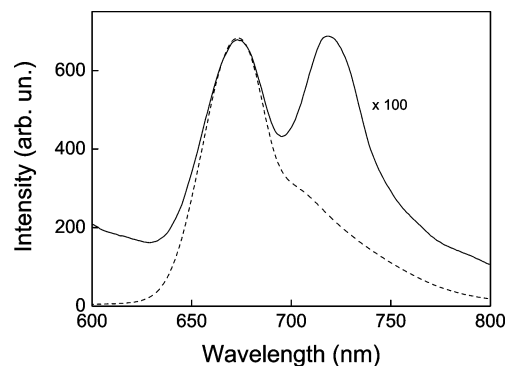


**Figure 8.** Fluorescence emission spectra of TPPS<sub>4</sub> in acidic methanol solution at different excitation wavelengths.  $\lambda_{ex} = 438$  nm (dashed line),  $\lambda_{ex} = 490$  nm (solid line).

the low quenching effect of alcohols. In Figure 8 the contribution of the fluorescence emission of S438 and S490 species is well identified.

The J-aggregate structure is mainly stabilized through electrostatic interactions between the negatively charged sulfonate groups and the positively charged nitrogen atoms of the porphyrin molecules and a network of hydrogen bonds. The involvement of H-bonds is highlighted by different spectroscopic features and aggregation kinetics, which are strictly connected with the polarity of the alcohols.

The aggregation process is extremely slow in methanol, sensitively faster in ethanol and almost instantaneous in both 1- and 2-propanol solutions. The different kinetic behaviors observed may be due to the decrease of the polarity that enhances the strength of interporphyrin H-bonding network and to the decreased porphyrin solubility that provides preformed nuclei thus promoting the aggregation process.<sup>2,15</sup> In particular, in methanol solution the self-organization of the chromophores is only partial and the UV/vis spectra evidence mainly shows the presence of a mixture of diacid form and J-aggregates, whereas in ethanol and propanol the complete disappearance of the monomer Soret band and the presence the J-aggregate (S490) and H-aggregate (S420) band only is observed. Time-resolved fluorescence spectroscopy confirms this picture, since a relative amplitude higher than 99% is observed for a lifetime shorter than 100 ps. The number of interacting monomers (coherence length) estimated from the comparison between the aggregate and monomer lifetimes<sup>39</sup> is in agreement with RLS results. The latter, according to the theory, show a resonant band which evidence the presence in solution of chromophore aggregates with coherence length higher than 20.<sup>20,37</sup>

In order to gain information on the size of such aggregates, QELS experiments in methanol have been carried out. The excess of light scattered intensity with respect to the solvent was slightly different from zero (above the experimental error) but no intensity autocorrelation function was detected. This occurrence could be ascribable to the presence in solution of small aggregates with hydrodynamic radius  $R_H$  less than 20 nm, which cannot be detected with the QELS measurements in the reported experimental conditions (micromolar concentrations). Unlike in the aqueous solutions, J-aggregates obtained in methanol have nanometric size that does not further evolve, while nanosized J-aggregates obtained in microemulsion water pools are unstable and macroscopically clusterize when continuous oil phase is removed.

## Conclusions

Alcoholic solutions of TPPS<sub>4</sub> show a peculiar behavior that mimics porphyrin in microemulsion confined water. Moreover,

these solutions evidence a metastable behavior, which has not been observed in bulk water and in other organic solvents.

In neutral fresh solution, the UV/vis absorption and time-resolved fluorescence measurements suggest the presence of small amounts of a dimeric species S400. In particular, for 1- and 2-propanol solutions UV/vis spectra show very broad absorption bands (due to the reduced solubility of TPPS<sub>4</sub>) and no resonant light scattering signal. In neutral aged solutions, a new species S423 appears in analogy with the species already observed in microemulsion water pools upon aging. For the methanol solutions, the interconversion kinetics between the species S415 and S423 is also highlighted by the gradual increase of the apparent initial fluorescence anisotropy. In acidic conditions, depending on the decreasing polarity of alcohol, a fast aggregation process takes place with the formation of J-aggregates (S490) (and H-aggregates) in close analogy with the species observed in confined water systems. The aggregation process is slow in methanol, faster in ethanol, and almost instantaneous in 1- and 2-propanol solutions. Such a process gives rise to small aggregates that are detectable in methanol by fluorescence measurements, but not observable by dynamic light scattering ( $R_H < 20$  nm).

There is a strict analogy between the spectroscopic features of alcohol solutions and those of confined water solutions (microemulsion pool) of TPPS<sub>4</sub>, both in neutral and acid form. Such an analogy can be attributed to the presence of amphiphilic interaction during the aggregate growth. The anionic TPPS<sub>4</sub> is present as monomer in highly polar solvent like water, but in the microemulsion water pool the amphiphilic contribution of the wall leads to the appearance of new species. By exploiting the amphiphilic character of short chain alcohols and by varying their polarity in a wide range, we could enhance, in bulk condition, the peculiar behavior observed in close proximity to the inner wall of the microemulsion.

**Acknowledgment.** We thank the FUSINT Project and MIUR (COFIN 2006) for financial support.

## References and Notes

- (1) Ribo, J.; Crusats, J.; Farrera, J.; Valero, M. *J. Chem. Soc., Chem. Commun.* **1994**, 681–682.
- (2) Castriciano, M. A.; Romeo, A.; Villari, V.; Micali, N.; Scolaro, L. M. *J. Phys. Chem. B* **2003**, *107*, 8765–8771.
- (3) Ohno, O.; Kaizu, Y.; Kobayashi, H. *J. Chem. Phys.* **1993**, *99*, 4128–4139.
- (4) Akins, D.; Zhu, H.; Guo, C. *J. Phys. Chem.* **1994**, *98*, 3612–3618.
- (5) Pasternack, R.; Schaefer, K.; Hambright, P. *Inorg. Chem.* **1994**, *33*, 2062–2065.
- (6) Maiti, N.; Ravikanth, M.; Mazumdar, S.; Periasamy, N. *J. Phys. Chem.* **1995**, *99*, 17192–17197.
- (7) Kano, H.; Kobayashi, T. *J. Chem. Phys.* **2002**, *116*, 184–195.
- (8) Micali, N.; Mallamace, F.; Romeo, A.; Purrello, R.; Scolaro, L. M. *J. Phys. Chem. B* **2000**, *104*, 5897–5904.
- (9) Micali, N.; Romeo, A.; Lauceri, R.; Purrello, R.; Mallamace, F.; Scolaro, L. M. *J. Phys. Chem. B* **2000**, *104*, 9416–9420.
- (10) Kano, H.; Kobayashi, T. *J. Lumin.* **2002**, *100*, 269–282.
- (11) Kano, H.; Kobayashi, T. *Bull. Chem. Soc. Jpn.* **2002**, *75*, 1071–1074.
- (12) Kano, H.; Saito, T.; Kobayashi, T. *J. Phys. Chem. A* **2002**, *106*, 3445–3453.
- (13) McRae, M.; Kasha, E. G. *Physical Processes in Radiation Biology*; Academic Press: New York, 1964.
- (14) Micali, N.; Villari, V.; Scolaro, L. M.; Romeo, A.; Castriciano, M. A. *Phys. Rev. E* **2005**, *72*, No. 050401.
- (15) Micali, N.; Villari, V.; Castriciano, M. A.; Romeo, A.; Scolaro, L. M. *J. Phys. Chem. B* **2006**, *110*, 8289–8295.
- (16) Maiti, N.; Mazumdar, S.; Periasamy, N. *J. Porphyrins Phthalocyanines* **1998**, *2*, 369–376.
- (17) Gandini, S.; Yushmanov, V.; Borissevitch, I.; Tabak, M. *Langmuir* **1999**, *15*, 6233–6243.
- (18) Maiti, N.; Mazumdar, S.; Periasamy, N. *J. Phys. Chem. B* **1998**, *102*, 1528–1538.
- (19) Castriciano, M. A.; Romeo, A.; Villari, V.; Angelini, N.; Micali, N.; Scolaro, L. M. *J. Phys. Chem. B* **2005**, *109*, 12086–12092.
- (20) Castriciano, M. A.; Romeo, A.; Villari, V.; Micali, N.; Scolaro, L. M. *J. Phys. Chem. B* **2004**, *108*, 9054–9059.
- (21) Pant, S.; Ohtaka-Saiki, H.; Takezaki, M.; Tominaga, T. *J. Mol. Liq.* **2001**, *90*, 121–130.
- (22) Smith, G. J. *Photochem. Photobiol.* **1985**, *41*, 123–126.
- (23) Micali, N.; Trusso, S.; Vasi, C.; Blaudez, D.; Mallamace, F. *Phys. Rev. E* **1996**, *54*, 1720–1724.
- (24) Petersen, M.; Voth, G. *J. Phys. Chem. B* **2006**, *110*, 7085–7089.
- (25) Dixit, S.; Crain, J.; Poon, W. C. K.; Soper, A. K.; Finney, J. L. *Nature* **2002**, *416*, 829.
- (26) Souda, R. *J. Phys. Chem. B* **2004**, *108*, 12159–12163.
- (27) Souda, R. *J. Phys. Chem. B* **2006**, *110*, 17524–17530.
- (28) Rivera, J.; McCabe, C.; Cummings, P. *Phys. Rev. E* **2003**, *67*, No. 011603.
- (29) De Luca, G.; Romeo, A.; Scolaro, L. M. *J. Phys. Chem. B* **2006**, *110*, 7309–7315.
- (30) Pasternack, R.; Collings, P. *Science* **1995**, *269*, 935–939.
- (31) Villari, V.; Micali, N. *J. Pharm. Sci.* **2008**, *97*, 1703–1730.
- (32) O'Connor, D. V.; Phillips, D. *Time-Correlated Single Photon Counting*; Academic Press: New York, 1984.
- (33) Lakowicz, J. R. *Principles of Fluorescence Spectroscopy*; Academic/Plenum Publishers: New York, 1999.
- (34) Angelini, N.; Micali, N.; Villari, V.; Mineo, P.; Vitalini, D.; Scamporrino, E. *Phys. Rev. E* **2005**, *71*, No. 021915.
- (35) Micali, N.; Mallamace, F.; Castriciano, M.; Romeo, A.; Scolaro, L. M. *Anal. Chem.* **2001**, *73*, 4958–4963.
- (36) Mazzaglia, A.; Angelini, N.; Lombardo, D.; Micali, N.; Patane, S.; Villari, V.; Scolaro, L. M. *J. Phys. Chem. B* **2005**, *109*, 7258–7265.
- (37) Parkash, J.; Robblee, J.; Agnew, J.; Gibbs, E.; Collings, P.; Pasternack, R.; De Paula, J. *Biophys. J.* **1998**, *74*, 2089–2099.
- (38) Akins, D.; Zhu, H.; Guo, C. *J. Phys. Chem.* **1996**, *100*, 5420–5425.
- (39) Akins, D.; Ozcelik, S.; Zhu, H.; Guo, C. *J. Phys. Chem.* **1996**, *100*, 14390–14396.

JP903430U